Neuroadaptations in the dorsal hippocampus underlie cocaine seeking during prolonged abstinence

Craig T. Werner[a,1,2], Swarup Mitra[a,1], Benjamin D. Auerbach[b,3], Zi-Jun Wang[a,3], Jennifer A. Martin[a], Andrew F. Stewart[a], Pedro H. Gobira[a,c], Madoka Iida[a], Chunna An[a], Moriah M. Cobb[a,d], Aaron Caccamise[a], Richard J. Salvi[b], Rachael L. Neve[e], Amy M. Gancarz[d], and David M. Dietz[a,f,2]

[a]Department of Pharmacology and Toxicology, Program in Neuroscience, Jacobs School of Medicine and Biomedical Sciences, The State University of New York at Buffalo, Buffalo, NY 14214; [b]Center for Hearing and Deafness, The State University of New York at Buffalo, Buffalo, NY 14214; [c]Department of Physics and Chemistry, School of Pharmaceutical Sciences of Ribeirão Preto, University of São Paulo, Ribeirão Preto, São Paulo, Brazil 14040; [d]Department of Psychology, California State University Bakersfield, Bakersfield, CA 93311; [e]Gene Delivery Technology Core, Massachusetts General Hospital, Cambridge, MA 02114; and [f]Department of Psychology, The State University of New York at Buffalo, Buffalo, NY 14260

Edited by Huda Akil, University of Michigan, Ann Arbor, MI, and approved September 3, 2020 (received for review April 2, 2020)

Relapse vulnerability in substance use disorder is attributed to persistent cue-induced drug seeking that intensifies (or "incubates") during drug abstinence. Incubated cocaine seeking has been observed in both humans with cocaine use disorder and in preclinical relapse models. This persistent relapse vulnerability is mediated by neuroadaptations in brain regions involved in reward and motivation. The dorsal hippocampus (DH) is involved in context-induced reinstatement of cocaine seeking but the role of the DH in cocaine seeking during prolonged abstinence has not been investigated. Here we found that transforming growth factor-β (TGF-β) superfamily member activin A is increased in the DH on abstinence day (AD) 30 but not AD1 following extended-access cocaine self-administration compared to saline controls. Moreover, activin A does not affect cocaine seeking on AD1 but regulates cocaine seeking on AD30 in a bidirectional manner. Next, we found that activin A regulates phosphorylation of NMDA receptor (NMDAR) subunit GluN2B and that GluN2B-containing NMDARs also regulate expression of cocaine seeking on AD30. Activin A and GluN2B-containing NMDARs have both previously been implicated in hippocampal synaptic plasticity. Therefore, we examined synaptic strength in the DH during prolonged abstinence and observed an increase in moderate long-term potentiation (LTP) in cocaine-treated rats compared to saline controls. Lastly, we examined the role of DH projections to the lateral septum (LS), a brain region implicated in cocaine seeking and found that DH projections to the LS govern cocaine seeking on AD30. Taken together, this study demonstrates a role for the DH in relapse behavior following prolonged abstinence from cocaine self-administration.

substance use disorder | relapse | dorsal hippocampus | ACTIVIN A | GluN2B

Substance use disorder (SUD) is a chronic disorder that is characterized by episodes of relapse despite long periods of drug abstinence (1). Relapse to drugs of abuse, such as cocaine, is often triggered by exposure to drug-associated cues that provoke drug seeking (2). Cue-induced cocaine seeking has been shown to progressively intensify (or "incubate") during prolonged periods of abstinence in individuals with cocaine use disorder (3, 4) and in preclinical relapse models (5–7).

Uncovering neuroadaptations that mediate persistent relapse vulnerability (8) holds potential for identifying novel pharmacotherapeutic targets to prevent and/or treat relapse. Neuroadaptations in the dorsal hippocampus (DH) have been observed in individuals with cocaine use disorder (9–12). Moreover, in preclinical models the DH has been shown to regulate context-induced reinstatement of cocaine seeking following self-administration and extinction of drug-reinforced responding (13–22). However, studies have not examined the role of the DH in relapse vulnerability during prolonged abstinence.

We have previously demonstrated an essential role for the transforming growth factor-β (TGF-β) superfamily signaling cascades in cellular and behavioral responses to cocaine (23–26) in the nucleus accumbens (NAc), a brain region that processes reward and motivated behaviors (27). TGF-β superfamily member activin A has been shown to be elevated in the NAc following a cocaine binge during abstinence (26). Activin A also mediates hippocampal synaptic plasticity through GluN2B-containing NMDA receptors (NMDARs) (28, 29) and GluN2B-containing NMDARs regulate context-induced reinstatement of cocaine seeking in the DH (15). Still, the roles of activin A and/or GluN2B in the DH in cocaine seeking during prolonged abstinence have not been examined.

In the present study, we found that following extended-access cocaine self-administration, activin A in the DH acquires an abstinent-dependent role in mediating cocaine seeking through a noncanonical mechanism that involves phosphorylation of

Significance

Achieving abstinence is difficult for individuals with cocaine use disorder but the greater challenge is avoiding relapse. Relapse vulnerability is provoked by exposure to drug-associated cues that evoke drug craving. Cue-induced drug craving persists during prolonged abstinence and is mediated by neuroadaptations in the brain. We found that activin A is increased in the dorsal hippocampus (DH) during prolonged, but not acute, abstinence and regulates phosphorylation of NMDA receptor subunit GluN2B. Both activin A and GluN2B-containing NMDA receptors in the DH regulate cocaine seeking during prolonged abstinence. Hippocampal synaptic strength is increased during prolonged abstinence and DH projections to lateral septum regulate cocaine seeking. Together, the DH acquires an abstinent-dependent role in regulating cocaine seeking during prolonged abstinence.

Author contributions: C.T.W., S.M., B.D.A., Z.-J.W., J.A.M., A.F.S., P.H.G., A.M.G., and D.M.D. designed research; C.T.W., S.M., B.D.A., Z.-J.W., J.A.M., A.F.S., P.H.G., M.I., C.A., M.M.C., A.C., and A.M.G. performed research; R.J.S. and R.L.N. contributed new reagents/analytic tools; S.M., B.D.A., Z.-J.W., P.H.G., M.M.C., and A.M.G. analyzed data; C.T.W., S.M., B.D.A., A.F.S., and D.M.D. wrote the paper; and R.J.S. provided support for LTP recordings.

The authors declare no competing interest.

This article is a PNAS Direct Submission.

See online for related content such as Commentaries.

[1]C.T.W. and S.M. contributed equally to this work.

[2]To whom correspondence may be addressed. Email: craig.werner@nih.gov or ddietz@buffalo.edu.

[3]B.D.A. and Z.-J.W. contributed equally to this work.

This article contains supporting information online at https://www.pnas.org/lookup/suppl/doi:10.1073/pnas.2006133117/-/DCSupplemental.

First published October 5, 2020.

GluN2B. We also observed an increase in hippocampal synaptic strength through the emergence of moderate LTP and determined that DH projections to the lateral septum (LS) regulate cocaine seeking during prolonged abstinence.

Results

Activin A Is Increased during Prolonged, but Not Acute, Abstinence in the DH following Cocaine Self-Administration. To examine activin A levels during abstinence, we utilized an extended-access cocaine

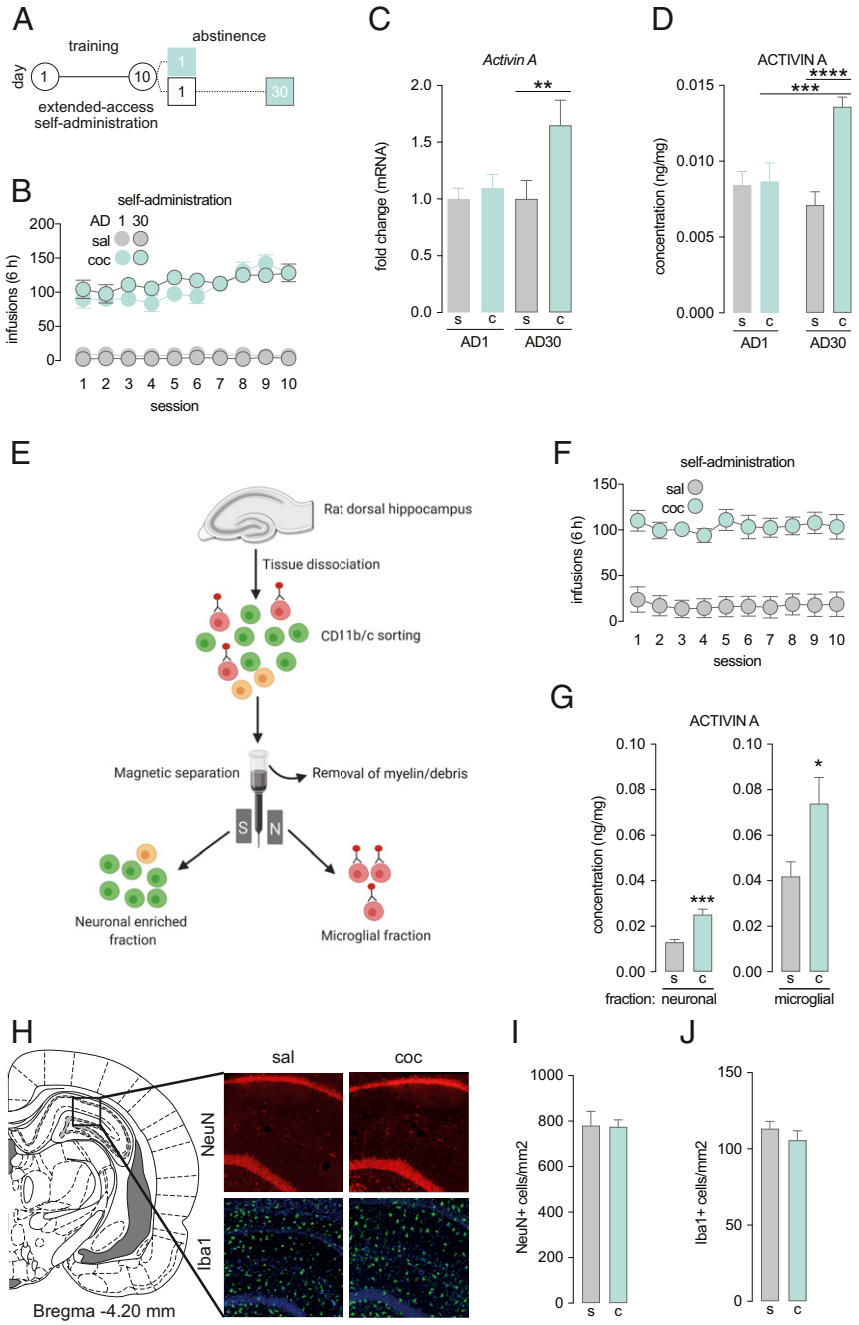

Fig. 1. Increased activin A expression in the DH at prolonged abstinence from cocaine self-administration. (*A*) Schematic of experimental timeline. (*B*) Self-administration training behavior (two-way repeated measures analyses of variance [ANOVA], cocaine groups: $F_{(1,17)} = 0.912$, $P = 0.353$, $n = 9$ to 10 rats/group). (*C*) *Activin A* gene expression (mRNA) in the DH during abstinence (two-way ANOVA, abstinence × treatment: $F_{(1,25)} = 5.965$, $P = 0.02$; Fisher's least significant difference [LSD] test: AD1 cocaine vs. AD30 cocaine, $P = 0.01$; AD30 saline vs. AD30 cocaine, $P = 0.008$; $n = 6$ to 8 rats/group). (*D*) ACTIVIN A protein concentrations in the DH during abstinence (two-way ANOVA, abstinence × treatment: $F_{(1,36)} = 11$, $P = 0.002$; Fisher's LSD test: AD1 cocaine vs. AD30 cocaine, $P = 0.001$; AD30 saline vs. AD30 cocaine, $P < 0.0001$; $n = 9$ to 12 rats/group). (*E*) Schematic for MACS sorting of DH tissues to obtain microglial and neuronal fraction (created with biorender.com). (*F*) Self-administration training behavior (two-way repeated measures ANOVA, treatment: $F_{(1,16)} = 30.88$, $P < 0.0001$, $n = 8$ to 10 rats/group). (*G*) ACTIVIN A protein concentrations in DH neuronal and microglial fractions (neuronal: *t* test, $t_{(15)} = 4.642$, $P = 0.0003$; microglial: *t* test, $t_{(16)} = 2.552$, $P = 0.021$; $n = 8$ to 10 rats/group). (*H*) Representative images of immunofluorescence staining in the DH at AD30 following cocaine (coc) or saline (sal) self-administration. (*I*) Cell density measurements represented as cells/mm^2 for NeuN and IBA1 immunoreactivity in the DH at AD30 following cocaine and saline self-administration (NeuN: *t* test $t_{(5)} = 0.07$, $P = 0.94$; IBA1+: $t_{(5)} = 0.91$, $P = 0.40$; $n = 3$ to 5 rats/group). $^*P < 0.05$; $^{**}P < 0.01$; $^{***}P < 0.001$; $^{****}P < 0.0001$. AD, abstinence day; sal/s, saline; coc/c, cocaine; N, north; S, south.

self-administration regimen wherein rats receive i.v. infusions of cocaine or saline paired with a light cue (30 and Fig. 1*B*). Following self-administration, rats underwent forced abstinence in home cages, which models incarceration or inpatient treatment (31). On abstinence day (AD) 1 or AD30, when incubated cue-induced cocaine seeking is expressed (5, 30), we collected DH tissue and then conducted an ELISA to quantify activin A concentrations (28). We found that *Activin A* mRNA and ACTIVIN A protein levels were increased in cocaine-treated rats on AD30, but not AD1, compared to the respective saline controls (Fig. 1 *C* and *D*). We then asked if activin A concentrations are affected by cue-induced cocaine seeking during prolonged abstinence. To answer this question (*SI Appendix*, Fig. S1*A*), rats underwent self-administration (*SI Appendix*, Fig. S1*B*) and then a cue-induced seeking test on AD30 (*SI Appendix*, Fig. S1*C*). We collected DH tissue 1 h following testing and found that ACTIVIN A was increased in cocaine-treated rats compared to saline controls (*SI Appendix*, Fig. S1*D*), suggesting that ACTIVIN A levels remain elevated independent of cocaine seeking. We also collected tissue from the NAc. In contrast to the DH (*SI Appendix*, Fig. S1*D*), we found no significant differences in ACTIVIN A in the NAc on AD30 (*SI Appendix*, Fig. S1*E*).

Because Activin A is expressed predominantly in neurons and microglia (26, 28, 32, 33), we sought to determine cell-type specificity of the source of activin A in the DH during prolonged abstinence. We first determined that abstinence from cocaine self-administration did not result in changes in neuronal (NeuN) or microglia (Iba1) immunoactivity in the DH (Fig. 1 *H–J*). This prompted us to turn to more sensitive and quantitative measures of cellular specificity to examine the cell-type-specific expression of ACTIVIN A at AD30. To achieve this, we trained rats to self-administer cocaine or saline (Fig. 1*F*). On AD30, we collected DH tissue and isolated neuronal and microglial fractions using magnetic-activated cell sorting (MACS) (Fig. 1*E*). We found that both DH neuronal and microglial fractions showed a significant increase in ACTIVIN A levels in cocaine-treated rats compared to saline controls (Fig. 1*G*), suggesting that multiple DH cell types contribute to the abstinent-dependent increase in activin A following cocaine self-administration.

Activin A Regulates Cocaine Seeking during Prolonged, but Not Acute, Abstinence. We then aimed to determine the functional role of activin A in cocaine seeking behavior during abstinence (Fig. 2*A*). Rats were trained to self-administer cocaine and were then pseudorandomly assigned to treatment groups based on cocaine infusions during training (Fig. 2*B*). On AD30, we injected anti-activin A antibody or IgG (IgG [control]) into guide cannula aimed at the CA1/CA3 subregions of the DH (Fig. 2*C*). Fifteen minutes after intra-DH injections, rats were returned to operant chambers for a cue-induced seeking test. We observed that blocking activin A in the DH significantly attenuated cue-induced cocaine seeking on AD30 compared to IgG controls (Fig. 2*D*).

To determine the neurobiological role of activin A in cocaine seeking during acute abstinence (Fig. 2*E*), we trained a separate group of rats (Fig. 2*F*) to test on AD1 when incubated seeking has not yet developed (5; Fig. 1*B*). In contrast to AD30, pretreatment with anti-activin A antibody did not affect cocaine seeking on AD1 (Fig. 2*G*), demonstrating that activin A mediates expression of cocaine seeking in an abstinent-dependent manner.

To test the reproducibility of our finding that blocking activin A attenuates cocaine seeking during prolonged withdrawal, we conducted an experiment using the endogenous activin bioneutralizer follistatin to inhibit activin A (34; *SI Appendix*, Fig. S3*A*). Following cocaine self-administration (*SI Appendix*, Fig. S2*B*), we found that an intra-DH injection of follistatin significantly decreased cocaine seeking compared to vehicle controls on AD30 (*SI Appendix*, Fig. S2*C*), providing additional support that activin A in the DH regulates cocaine seeking during prolonged abstinence.

We then asked if activin A regulates cocaine seeking in a bidirectional manner (Fig. 2*I*). To test this, we utilized viral-mediated gene transfer to overexpress activin A Receptor Type 2a (ACVR2A) or GFP (green fluorescent protein [control]) in DH neurons, where endogenous activin receptors are expressed (28). Following cocaine self-administration (Fig. 2*I*), rats were pseudorandomly assigned to receive herpes simplex virus (HSV)-*ACVR2A* or HSV-*GFP* (control) on AD27. On AD30, when viruses are maximally expressed (35), we tested cue-induced cocaine seeking and found that viral-mediated overexpression of ACVR2A increased cocaine seeking compared to GFP controls (Fig. 2*J*). Importantly, manipulating activin A signaling did not affect locomotor activity (*SI Appendix*, Fig. S3 *A* and *B*). Together, these data suggest that activin A in the DH bidirectionally regulates expression of cocaine seeking during prolonged abstinence.

Phosphorylated GluN2B Is Increased in the DH and GluN2B-Containing NMDARs Govern Cocaine Seeking during Prolonged Abstinence. Activin A has been shown to modulate hippocampal synaptic activity via phosphorylation of NMDAR subunit GluN2B (28, 29). Therefore, we next examined expression of GluN2B in the DH on AD30. We found an increase in phosphorylated (p)-GluN2B, while total GluN2B was unchanged, in cocaine-treated rats compared to saline controls (Fig. 3*A*). Activin A-induced phosphorylation of GluN2B and LTP are believed to be driven by extracellular signal-regulated kinase/mitogen-activated protein kinase (ERK/MAPK) (28), which may involve Ras-GRF1, a Ca^{2+}/calmodulin-dependent Ras-guanine-nucleotide-releasing factor that regulates GluN2B (36). We found that, similar to p-GluN2B, Ras-GRF1 expression was also increased on AD30 in cocaine-treated rats compared to saline controls (Fig. 3*A*). Next, we examined GluN2B surface and intracellular expression. Using a biotinylated assay, we observed that surface expression of GluN2B was increased, while intracellular GluN2B was decreased, in the DH of cocaine-treated rats compared to saline controls (Fig. 3*B*). Importantly, we also found that blocking activin A reduced p-GluN2B but not total GluN2B in cocaine-treated rats on AD30 (Fig. 3*C*), suggesting that the increase in p-GluN2B in cocaine-treated rats is regulated, at least in part, by activin A signaling.

We next examined the role of GluN2B in cocaine seeking during prolonged abstinence (Fig. 3*D*). Rats were trained to self-administer cocaine (Fig. 3*E*) and then on AD30 we injected Ro 25-6981, a GluN2B-containing NMDAR antagonist (37), or vehicle into the DH 15 min prior to testing. Pharmacological inhibition of GluN2B-containing NMDARs reduced cocaine seeking compared to vehicle controls (Fig. 3*F*), suggesting that, in addition to activin A, GluN2B-containing NMDARs in the DH also contribute to expression of cocaine seeking during prolonged abstinence.

Previous studies have demonstrated that activin A mediates moderate LTP in the hippocampus via GluN2B-containing NMDARs (28, 29). We observed increased activin A concentration (Fig. 1*D*), p-GluN2B expression (Fig. 3*A*), and surface GluN2B expression (Fig. 3*C*) in the DH, leading us to hypothesize that moderate LTP may be enhanced during prolonged abstinence following cocaine self-administration. To test this hypothesis (*SI Appendix*, Fig. S4*A*), we trained rats to self-administer cocaine (*SI Appendix*, Fig. S4*B*) and then measured LTP upon weak theta-burst stimulation (TBS) in the CA1 region of acute hippocampal slices (28) during abstinence. Interestingly, we found that weak TBS induced moderate LTP in slices from cocaine-treated rats but not saline controls (*SI Appendix*, Fig. S4 *C* and *D*). Importantly, we found no differences in I/O (input/output)

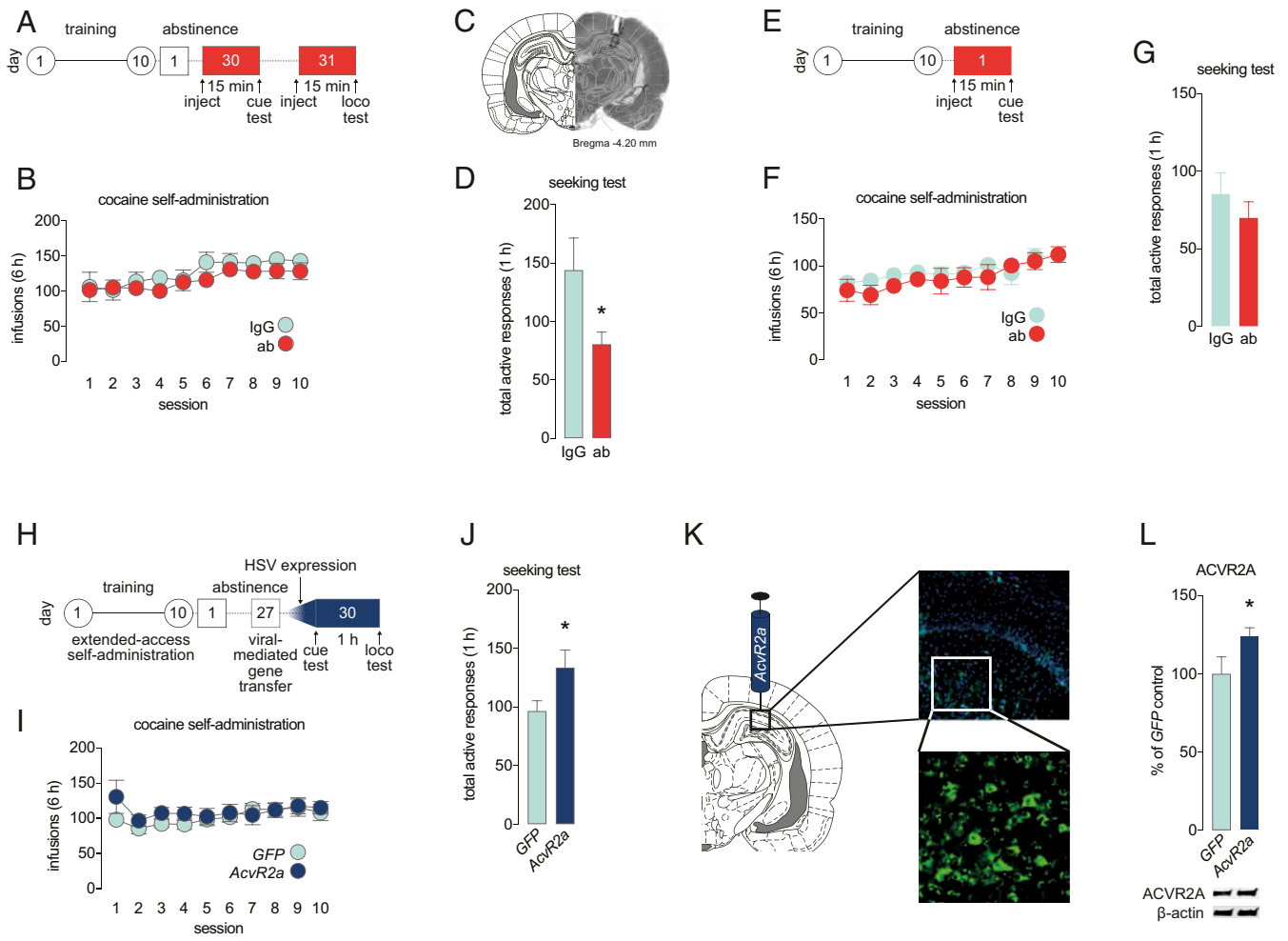

Fig. 2. Activin A in the DH bidirectionally regulates cocaine seeking during prolonged abstinence. (*A*) Schematic of experimental timeline. (*B*) Cocaine self-administration training behavior prior to pharmacological manipulation on AD30 (two-way repeated measures ANOVA, treatment: $F_{(1,11)} = 0.331$, $P = 0.577$, $n = 6$ to 7 rats/group). (*C*) Representative photomicrograph of microinfusion cannula placement. (*D*) Total active responses during a cue-induced seeking test on AD30 (*t* test, $t_{(11)} = 1.973$, $P = 0.037$; $n = 6$ to 7 rats/group). (*E*) Schematic of experimental timeline for AD1 pharmacological manipulation. (*F*) Cocaine self-administration training behavior prior to pharmacological manipulation on AD1 (two-way repeated measures ANOVA, treatment: $F_{(1,15)} = 2.005$, $P = 0.1777$, $n = 8$ to 9 rats/group). (*G*) Total active responses during a cue-induced seeking test on AD1 (*t* test, $t_{(15)} = 0.353$, $P = 0.729$; $n = 8$ to 9 rats/group). (*H*) Schematic of experimental timeline. (*I*) Cocaine self-administration training behavior prior to viral-mediated gene transfer on AD30 (two-way repeated measures ANOVA, treatment: $F_{(1,11)} = 0.65$, $P = 0.437$, $n = 5$ to 8 rats/group). (*J*) Total active responses during a cue-induced seeking test (*t* test, $t_{(25)} = 2.068$, $P = 0.024$; $n = 12$ to 15 rats/group). (*K*) Anatomical placement of viral infection and representative image of HSV-infected area in the DH. (*L*) Acvr2a protein expression in DH tissue infected with HSV-Acvr2a ($t_{(10)} = 1.977$, $P = 0.03$; $n = 6$ rats/group). *$P < 0.05$. AD, abstinence day; sal/s, saline; coc/c, cocaine; ab, antibody; HSV, herpes simplex virus; loco, locomotion; GFP, green fluorescent protein.

or PPR (paired-pulse ratio) (*SI Appendix*, Fig. S4 *D* and *E*) between groups, indicating that cocaine treatment did not significantly alter basal synaptic transmission in the hippocampal CA1 region. At the end of recording days, we collected unused acute hippocampal slices from the oxygenated chamber and found increased ACTIVIN A concentration in slices from cocaine-treated rats compared to saline controls (*SI Appendix*, Fig. S4*G*). This replicates our findings (Fig. 1*D*) and provides a correlational link between ACTIVIN A and moderate LTP in the DH.

DH Projections to LS Regulate Cocaine Seeking during Prolonged Abstinence. We determined that, during prolonged abstinence, activin A and GluN2B-containing NMDARs in DH CA1/CA3 regulate cue-induced cocaine craving and that weak TBS stimulation of the Schaffer collaterals produces moderate LTP in CA1. Next, we sought to examine circuitry involving the DH that contributes to cocaine-seeking behavior. The DH sends projections to the LS (38–40), a brain region that is involved in cue- and context-induced cocaine seeking (17). To test whether DH inputs to LS regulate cue-induced cocaine seeking on AD30, we used chemogenetic tools to silence DH neurons that project to the LS. After cocaine self-administration (Fig. 4*B*), we expressed retrograde adeno-associated virus (AAVretro)-Cre-GFP (retro-Cre) or AAV-Cre-GFP (Cre) in the LS and DIO-hM4D(Gi) (designer receptor exclusively activated by designer drugs [DREADD]) in the DH (Fig. 4*E*). On AD30, all rats received an injection of clozapine-*N*-oxide (CNO; 1 mg/kg, i.p.) and 30 min later were returned to the operant chamber for a seeking test (Fig. 4*A*). Chemogenetic inhibition of DH inputs to LS significantly attenuated cocaine seeking (Fig. 4*C*). Two hours following the test, we perfused rats and observed a decrease in LS fos-positive cells in retro-Cre rats compared to Cre controls (Fig. 4*D*), confirming DREADD-mediated silencing of DH-to-LS projection neurons. These findings suggest that DH inputs

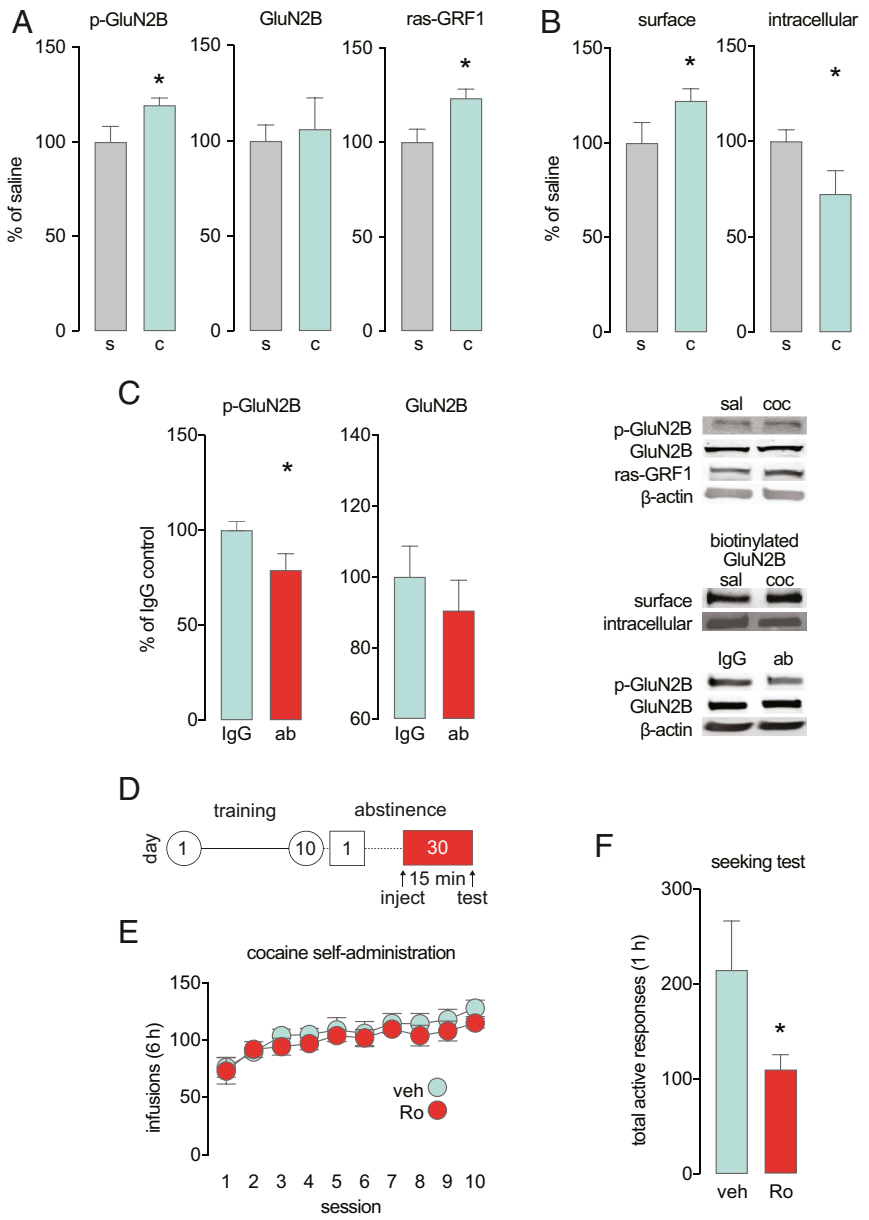

Fig. 3. DH GluN2B-containing NMDARs regulate cocaine seeking during prolonged abstinence. (*A*) DH protein expression for (ab) p-GluN2B (*Left* bars; *t* test, $t_{(17)} = 1.885$, $P = 0.038$; $n = 8$ to 11 rats/group), total GluN2B (*Middle* bars; *t* test, $t_{(10)} = 0.326$, $P = 0.751$; $n = 6$ rats/group), and ras-GRF1 (*Right* bars; *t* test, $t_{(16)} = 2.616$, $P = 0.019$; $n = 8$ to 10 rats/group). DH protein expression for (*B*) surface GluN2B (*Left* bars; *t* test, $t_{(13)} = 1.717$, $P = 0.055$; $n = 7$ to 8 rats/group) and intracellular GluN2B (*Right* bars; *t* test, $t_{(13)} = 2.099$, $P = 0.028$; $n = 7$ to 8 rats/group). (*C*) DH protein expression for (*Left* bars) p-GluN2B and (*Right* bars) total GluN2B following intra-DH injections of anti-activin A antibody or IgG (p-GluN2B: *t* test, $t_{(9)} = 2.0$, $P = 0.038$; $n = 5$ to 6 rats/group; GluN2B: *t* test, $t_{(9)} = 0.789$, $P = 0.462$; $n = 5$ to 6 rats/group). (*D*) Schematic of experimental timeline. (*E*) Cocaine self-administration training behavior prior to pharmacological manipulation (two-way repeated measures ANOVA, treatment: $F_{(1,12)} = 0.569$, $P = 0.465$, $n = 7$ rats/group). (*F*) Total active responses during a cue-induced cocaine-seeking test on AD30 (*t* test, $t_{(12)} = 1.964$, $P = 0.037$; $n = 7$ rats/group). *$P < 0.05$. s/sal, saline; c/coc, cocaine; veh, vehicle; Ro, Ro 25-6981.

to LS are required for expression of cocaine seeking during prolonged abstinence.

Discussion

Here we demonstrate that activin A signaling in the DH regulates cocaine-induced neuroadaptations and expression of cue-induced cocaine seeking during prolonged abstinence. We found that DH activin A levels were significantly increased on AD30, but not AD1, in cocaine-treated rats compared to saline controls. Using pharmacological, viral, and biochemical approaches, we determined that activin A signaling bidirectionally regulates cocaine seeking during prolonged abstinence through a process that involves GluN2B-containing NMDARs (*SI Appendix*, Fig. S5). We then more broadly characterized DH neuroadaptations during prolonged abstinence. We demonstrated that cocaine induces moderate LTP in the DH and that DH–LS projections regulate cocaine seeking during prolonged abstinence.

The DH has previously been implicated in context-induced reinstatement of cocaine seeking and associated memory reconsolidation. In some studies, rats were trained to self-administer cocaine in a distinct, cocaine-paired context. Responding was then extinguished in an alternate context, followed by reinstatement of

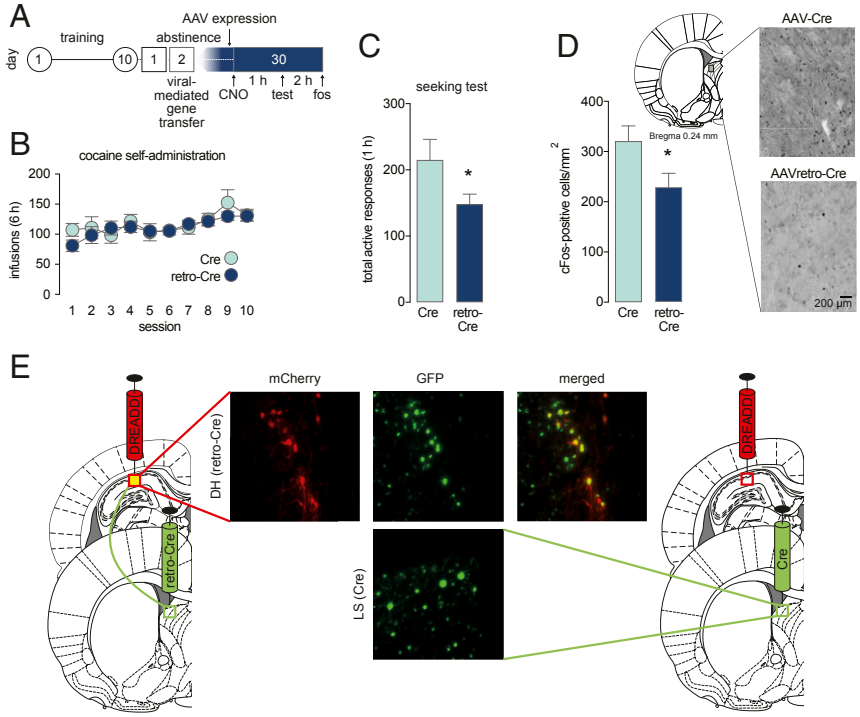

Fig. 4. DH projections to LS regulates cocaine seeking during prolonged abstinence. (*A*) Schematic of experimental timeline. (*B*) Cocaine self-administration training behavior prior to viral-mediated gene therapy (two-way repeated measures ANOVA, virus: $F_{(1,17)} = 0.209$, $P = 0.654$, $n = 9$ to 10 rats/group). (*C*) Total active responses during a cue-induced cocaine-seeking test 30 min after systemic CNO injection on AD30 (*t* test, $t_{(17)} = 1.966$, $P = 0.033$; $n = 9$ to 10 rats/group). (*D*) Fos-positive cells in the LS 2 h after cue-induced seeking test (*t* test, $t_{(12)} = 2.239$, $P = 0.045$; $n = 2$ slices/rat, 7 rats/group). (*E*) Schematic representation of DREADD procedure for DH–LS circuit inhibition and representative images of AAV DREADD infection in DH, AAV-cre infection in LS, and AAV-retro CRE and DREADD colocalization in the DH. *$P < 0.05$. DREADD, Designer Receptor Exclusively Activated by Designer Drugs; AAV, adeno-associated virus; CNO, clozapine-*N*-oxide; retro, retrograde.

cocaine seeking in the drug-paired context (13, 15–17, 19, 21, 22). In other studies, rats were briefly reexposed to the cocaine-paired context following extinction to reactivate cocaine-associated memories before undergoing additional extinction and reinstatement testing (14, 18, 20). These studies found that the DH regulates context-induced reinstatement of cocaine seeking (13, 15–17, 19, 21, 22), as well as reconsolidation of memories that maintain context-induced cocaine seeking (14, 18, 20). Interestingly, previous studies reported that the DH is not involved in cue-induced and/or cocaine-primed reinstatement (13, 17). It is important to note that there is no prolonged abstinence period between self-administration training, extinction training, and reinstatement testing in these studies. Additionally, these studies used short-access self-administration procedures, which produce different cellular and behavioral plasticity compared to extended-access procedures (30, 41–43). Lastly, extinction training itself also induces neuroadaptations (44), which can be difficult to separate from those elicited by abstinence and relapse (45).

The hippocampus proper is comprised of four subregions, cornus ammonis 1 (CA1), CA2, CA3, and CA4. Previous studies have implicated CA1/CA3 (13–15) and CA3 (16, 17), but not the overlying cortex and adjacent dentate gyrus (13, 46), in drug context-induced reinstatement of cocaine seeking. Our study focused on the CA1/CA3 subregions of the DH. We found that the DH is not involved in cue-induced cocaine seeking during acute abstinence (AD1), which aligns with previous studies that found that the DH is not involved in cue-induced reinstatement of cocaine seeking after extinction (13, 17). However, we observed that the DH acquires an abstinent-dependent role in regulating cocaine seeking during prolonged abstinence (AD30). This study adds to a growing body of literature characterizing temporally dynamic, cocaine-induced plasticity that occurs during abstinence that may contribute to perpetual relapse vulnerability (8, 30, 47–53).

Activin A is a member of the TGF-β superfamily. Previously, we have demonstrated roles for TGF-β signaling in the NAc in cocaine-induced plasticity and relapse behaviors. TGF-β family member Smad3, a transcription factor, and BRG1, a core subunit of the SWI/SNF chromatin remodeling complexes family that interacts with Smads, mediate cocaine reinstatement (23, 24). Moreover, we found that activin A was increased following a cocaine binge during abstinence, which may be mediated by activated microglia (26). Activin A has also been shown to mediate hippocampal synaptic plasticity and memory (28, 29, 54, 55), but the role of Activin A in SUD-related behaviors had not previously been examined. Here we found an abstinent-dependent increase in Activin A in the DH that regulates expression of cocaine seeking during prolonged abstinence. We performed magnetic-activated cell sorting with DH tissue on AD30 and found increased Activin A concentrations in both microglia and neuronal fractions, suggesting that multiple cell types contribute to the increase in Activin A concentration on AD30 in cocaine-treated rats compared to saline controls. These findings generally corroborate previous observations in which ACTIVIN is expressed in both glutamatergic neurons and glial cells in the DH, although greater expression was observed in neurons (28). Previous studies also reported that the hippocampus is one of the most densely populated regions of Activin receptors in the brain (56) and that Activin receptors are primarily expressed in neurons (28). We found that manipulating Activin A signaling in the DH bidirectionally regulates cocaine seeking during prolonged, but not acute, abstinence.

Activin A modulates hippocampal plasticity through GluN2B (28, 29) and GluN2B-containing NMDARs in the DH have been

implicated in context-induced reinstatement of cocaine seeking (15). Xie et al. (15) demonstrated that pharmacological blockade of GluN2B-containing NMDARs via intra-DH Ro 25-6981 treatment reduced active lever responding in a cocaine-paired context. Importantly inhibiting GluN2B-containing NMDARs did not affect active lever responding in an extinction context and also did not alter locomotor activity or food-reinforced responding. In our study, we found that p-GluN2B and surface GluN2B are increased in the DH on AD30 following cocaine self-administration, and antagonizing GluN2N-containing NMDARs attenuates cue-induced cocaine seeking on AD30. Moreover, we found that inhibiting Activin A signaling reduced p-GluN2B, suggesting that the phosphorylation of GluN2B we observed is at least partly regulated by ACTIVIN A. ACTIVIN A has been implicated in synaptic hippocampal transmission, including moderate LTP, via phosphorylation of GluN2B (28, 29). While observations of cocaine-induced hippocampal LTP during abstinence are inconsistent (57, 58), we found that extended-access cocaine self-administration produces an increase in moderate LTP in the DH on AD30. We also observed that ACTIVIN A concentration was increased in unused acute hippocampal slices from cocaine-treated rats during prolonged abstinence compared to saline controls. While not causational, these data suggest that ACTIVIN A may be involved in cocaine-induced LTP in the DH following prolonged abstinence. Future studies will be required to demonstrate a cellular role for ACTIVIN A in mediating hippocampal LTP following cocaine exposure.

The DH sends projections to multiple brain regions, including the LS (38–40). DH CA3-to-LS projections have previously been implicated in context-, but not cue-induced reinstatement of cocaine seeking (16, 17). We found that DH-to-LS projections regulate cue-induced cocaine seeking during prolonged abstinence. Contextual cues likely contribute to the cocaine seeking we measure in our model, as we do not extinguish rats to the context. However, our observed abstinent-dependent effect of ACTIVIN A in the DH suggests that the DH undergoes neuroadaptations during abstinence, and therefore, circuit adaptations during abstinence are also very likely.

Together, our findings demonstrate roles for ACTIVIN A and the temporally dependent emergence of the DH in mediating relapse vulnerability during prolonged abstinence, which provide directions for the development of pharmacotherapies for the treatment of substance use disorder.

Methods

Subjects. This study was conducted in accordance with the guidelines set up by the Institutional Animal Care and Use Committee of The State University of New York at Buffalo. Adult male Sprague–Dawley rats (250 to 275 g; Envigo) were maintained on a 12-h reverse light/dark cycle and allowed ad libitum access to food and water. Following 5 to 7 d to habituate to the colony room, i.v. jugular catheters were implanted and rats were singly housed.

Drugs. (–)-Cocaine hydrochloride, generously supplied by the National Institute on Drug Abuse drug supply program, was dissolved in sterile 0.9% saline. Cocaine solutions were prepared on a weekly basis and delivered via syringe pump. Pump durations/injection volumes were adjusted on a daily basis according to body weight. The following drugs were used for intracranial injections: anti-Activin A antibody (0.667 μg/μL; R&D Systems; AF338) dissolved in 1× phosphate-buffered saline (PBS) (54); follistatin (0.5 μg/μL; R&D Systems; 4889-FN) dissolved in 0.1% bovine serum albumin (BSA) in 1× PBS (54); Ro 25-6981 (0.5 nmol/μL; Millipore; R7150) dissolved in 0.9% sterile saline (59).

Jugular Catheterization and Patency Testing. Rats were implanted with chronic indwelling jugular catheters as described previously with minor modifications (60). Rats were allowed 5 d to recover following surgery. The catheters were flushed daily with 0.2 mL of a solution of enrofloxacin (4 mg/mL) in heparinized saline (50 IU/mL in 0.9% sterile saline) to preserve catheter patency. The day before behavioral training, each animal received an i.v. infusion of ketamine hydrochloride (0.5 mg per kg in 0.05 mL) and the behavioral response (loss of muscle tone and righting reflexes) were observed to verify catheter patency. Only rats with patent catheters were used in behavioral studies (<1% of animals tested for self-administration were excluded from the experiment due to loss of patency).

Acquisition of Self-Administration. Following recovery from jugular catheter surgery, rats were randomly assigned to train to self-administer cocaine or saline as previously described (61). Briefly, operant chambers were equipped with two nose poke holes (MED Associates) in sound-attenuating cabinets. Responses in the active hole resulted in an infusion using a fixed ratio (FR)1 schedule of reinforcement, which was increased daily to FR5. Infusions were accompanied by a 5-s illumination of the cue light above the active hole and the house light was extinguished for the duration of the infusion and 30-s timeout period. Responses in the inactive hole resulted in no consequences but were recorded. The criterion for acquisition of cocaine self-administration was an average of eight infusions/session during the last three acquisition sessions.

Extended-Access Self-Administration. Following self-administration acquisition, rats were allowed to self-administer cocaine (0.5 mg/kg/infusion [(1.75 mg/mL × 198 cS infusion for 275 g rat]) or saline for 10 d under an extended-access regimen (6 h/day) using a FR5 schedule of reinforcement as we have previously described (26, 61). Following training sessions, catheters were flushed and rats were returned to the colony room. Only rats that reached acquisition criterion and responded for cocaine (an average of ≥50 infusions/session for ≥5 consecutive days) were used in successive phases of experiments (30). We report drug infusions in figures and active and inactive responses for training behavior in *SI Appendix*, Table S1.

Pharmacological Manipulations. Rats received jugular catheters and implantation of custom bilateral guide cannulas (Plastics One, Inc.) that were aimed at the CA1 of the DH (coordinates from bregma according to ref. 62: anterior/posterior (AP): −4.2; medial/lateral (ML): 3; dorsal/ventral (DV): −3) (63). Animals were assigned to receive microinjections (1 μL/hemisphere) infused at a rate of 0.2 μL/min; injectors were left in place for an additional 5 min to allow for diffusion. Fifteen minutes after the microinjection (54), animals were tested for cue-induced seeking.

Viral-Mediated Gene Transfer. The plasmid pDONR223-ACVR2A, a gift from William Hahn and David Root, Addgene, Cambridge, MA (Addgene plasmid 23654) (64), was used to make a herpes simplex virus (HSV) vector. HSV vectors were generated in p1005 transcription cassettes expressing green fluorescent protein (GFP) driven by a CMV promoter to allow for neuronal visualization. Such HSV vectors exhibit maximal expression 3 to 5 d postinjection (35). All viral tools were validated before use in behavioral experiments. Injectors were aimed at the CA1 region of the DH with a 10° angle (AP: −4.36 mm; ML: 3.4 mm; DV: −2.4 mm) and virus was manually infused at a rate of 0.2 μL/min for a total of 1 μL/hemisphere. All viral tools were validated in vivo using immunofluorescence (anti-rabbit GFP, 1:1,000; Life Technologies; A11122) and immunoblotting (anti-rabbit AcvR2a, 1:1,500; Abcam; ab134082).

Cue-Induced Seeking Test. Rats were returned to operant chambers to measure cue-induced seeking. Tests were performed under extinction conditions (i.e., responses in the active hole delivered the infusion-paired cue light but no infusion) and lasted 1 h as previously described (25). The total number of responses in the active hole was the operational measure of seeking from which the affective state of craving was inferred (51). We report total active responses in figures and total inactive responses for seeking test behavior in *SI Appendix*, Table S2.

Locomotor Activity. Locomotor activity was quantified in transparent plastic cages fitted with an infrared motion-sensor system (Omnitech Electronics, Inc.) using VersaMax animal activity software (Omnitech Electronics, Inc.) that monitors distance traveled. Locomotor activity was recording during a 1-h test.

Tissue Collection and Homogenization. Tissue was collected during abstinence after self-administration training. Following rapid decapitation, brains were removed and sliced into 1-mm-thick sections using a brain matrix and the DH and NAc were collected and rapidly frozen on dry ice for biochemical experiments or immediately processed for cell-type separation.

ELISA. Frozen DH dissections were homogenized in buffer (0.32 M sucrose, 5 mM Tris·HCl [pH 8.0], protease inhibitor tablet) (Hoffman-La Roche; 11836170001) and homogenates were then centrifuged at 20,000 × *g* at 4 °C. Activin A concentrations were quantified using the Quantikine Activin A Immunossay (R&D Systems, Inc.; DAC00B) according to manufacturer's instructions and as previously described (26, 28, 65).

RNA Isolation and qPCR. Quantification of *Activin A* mRNA in the DH was performed as previously described (30). Briefly, bilateral DH tissue punches were collected from animals that self-administered cocaine or saline at AD30 and RNA was extracted using TRIzol reagent (Ambion) and purified with the E.Z.N.A. MicroElute Total RNA Kit (Omega Bio-Tek). RNA concentration was then measured on a NanoDrop One spectrophotometer (Thermo Scientific) and reverse transcribed using the SuperScript III First-Strand Synthesis System (Invitrogen). mRNA expression for Activin A was quantified using qPCR with IQ SYBR Green SuperMix (Bio-Rad Laboratories) in a CFX384 System (Bio-Rad Laboratories). All reactions were run in triplicates and threshold cycles (Ct) were analyzed by a relative quantification method (ΔΔCt) against *Gapdh* as a housekeeping gene. For *Activin A*, the primer sequences used were 5′-GAG GACGACATTGGCAGGAG-3′ (forward) and 5′-CGCTGGATGCTGCTAGACAC-3′ (reverse) and for *GAPDH* the sequences were 5′-AACGACCCCTTCATTGAC-3′ (forward) and 5′-TCCACGACATACTCAGCA-3′ (reverse).

Immunoblotting. Protein concentrations were determined, and 20 to 30 μg of protein/lane was loaded onto 10% Tris-sodium dodecyl sulfate (SDS) polyacrylamide gels for electrophoresis (PAGE) separation and then transferred to nitrocellulose membranes, blocked with Rockland Blocking Buffer (Rockland; MB-070), and incubated overnight at 4 °C with primary antibodies diluted in Rockland Blocking Buffer: anti-phosphorylated (p)-GluN2B (1:1,000; Millipore; AB5403) (66), anti-GluN2B (1:500; Millipore; 06-600) (67) and anti-β-actin (loading control; 1:10,000; Cell Signaling Technology; 3700) (25). After washes with Tris-buffered saline with Tween-20 (TBS-T; TBS containing 0.1% Tween-20), membranes were incubated with IRDye secondary antibodies (1: 5,000; LI-COR; 926-68072) in Rockland Blocking Buffer for 1 h at room temperature (RT). Blots were then imaged using the Odyssey Infrared Imaging System (LI-COR) and quantified by densitometry using ImageJ (NIH).

Magnetic-Activated Cell Sorting. Neuronal and microglial fractions were separated using MACS Cell Separation (Miltenyi Biotec) as per manufacturing instructions with minor modifications. Briefly, rats were rapidly decapitated and brains were removed and sliced into 1-mm-thick sections using a brain matrix and the DH was dissected and cut into small pieces in 1× PBS using a scalpel. Tissue was then rinsed with 1× PBS, centrifuged at 300 × *g* for 2 min at RT and the supernatant was aspirated. Next, preheated enzyme mix 1 was added and incubated in closed tubes for 15 min at 37 °C at 300 rpm and then enzyme mix 2 was added to samples and inverted gently. Tissue was then dissociated mechanically using a wide-tipped, fire-polished Pasteur pipette and incubated at 37 °C for 10 min at 300 rpm. Two fire-polished pipettes in decreasing diameter were then used to further dissociate tissue before incubating again at 37 °C for 10 min at 300 rpm. Next, the cell suspension was applied to a prewetted MACS SmartStrainer filter (Miltenyi Biotec; 130-098-462) placed in a 1.7-μL microcentrifuge tube. Collected flowthrough was then centrifuged at 300 × *g* for 10 min at RT and supernatant aspirated. Myelin was then removed from the cell suspensions due to the large amount of myelination in the adult rat hippocampus. To do so, 1× PBS and Myelin Isolation Beads (Miltenyi Biotec; 130-104-257) were added to the aspirated supernatant, mixed, and incubated for 15 min at 4 °C. MS Columns (Miltenyi Biotec; 130-042-201) were placed on a magnetic OctoMACS separator (Miltenyi Biotec; 130-042-109) on a MACS MultiStand (Miltenyi Biotec; 130-042-303) and rinsed with 1× PBS before cell suspensions were applied onto the columns. Unlabeled fractions were collected and centrifuged at 300 × *g* 4 °C for 10 min. Aspirated supernatants were then resuspended in 1× PBS and CD11b/c MicroBeads (Miltenyi Biotec;130-105-643), mixed, and incubated for 15 min at 4 °C. Next, cells were washed and centrifuged at 300 × *g* for 10 min and supernatants were aspirated and resuspend in 1× PBS. MS Columns were then placed on the OctoMACS, washed, and cell suspensions were applied. The flowthrough was collected (neuronal fraction), and the column was removed from the separator and flushed with 1× PBS with the column plunger to collect microglial fractions. Fractions were then centrifuged at 14,000 × *g* at 4 °C for 10 min and resuspended in radioimmunoprecipitation assay (RIPA) buffer.

Biotinylation. Biotinylation assay was conducted as previously described with minor modifications (68). Briefly, frozen DH tissue was minced in microcentrifuge tubes containing cold artificial cerebrospinal fluid (aCSF) and sulfosuccinimidyl-2-(biotinamido)ethyl-1,3-dithiopropionate (Sulfo-NHS-SS-Biotin; Thermo Scientific; PG82077) followed by quenching with 100 mM glycine and centrifuged. Tissue was then pelleted and fractions were resuspended in ice cold lysis buffer containing protease inhibitor mixture (Roche), sonicated, and stored at −80 °C. A total of 100 μg of each sample was incubated overnight with 37.5 μg of NeutrAvidin beads (Thermo Scientific; 29204) to isolate bound and unbound fractions. The bound fraction comprised of biotinylated proteins (surface expression) was separated from the unbound material containing nonbiotinylated proteins by centrifugation (3,000 rpm for 1 min) and washing with ice cold 1× PBS. Both fractions were heated at 97 °C following treatment with 2× laemmli buffer and 200 mM dithiothreitol (DTT), centrifuged, and supernatant (35 μg protein/sample) was analyzed in SDS/PAGE.

Slice Preparation. Rats on AD30 to 47 were deeply anesthetized, perfused with ice-cold dissection buffer containing (in mM): NaCl 87, sucrose 75, KCl 2.5, NaH_2PO_4 1.25, $NaHCO_3$ 25, $CaCl_2$ 0.5, $MgCl_2$ 7, ascorbic acid 1.3, and D-glucose 10 (saturated with 95% O_2 to 5% CO_2) and then decapitated. Transverse hippocampal slices (350 μm thick) were prepared in ice-cold dissection buffer using a vibrating microtome (VF-200 Compresstome, Precisionary Instruments). Immediately following slicing, the CA3 region was removed. Slices were recovered in aCSF containing (in mM): NaCl 124, KCl 5, NaH_2PO_4 1.23, $NaHCO_3$ 26, $CaCl_2$ 2, $MgCl_2$ 1, and D-glucose 10 (saturated with 95% O_2 to 5% CO_2) at 30 °C for ≥1 h prior to recording.

Electrophysiology. Field recordings were performed in a submersion chamber (Harvard Apparatus), perfused with aCSF (2 to 3 mL/min) at 30 °C. Field excitatory postsynaptic potentials (fEPSPs) were recorded extracellularly in CA1 stratum radiatum using glass electrodes (1 to 2 MΩ) filled with aCSF. Synaptic responses were evoked by stimulation of the Schaffer collaterals with a 0.2-ms pulse delivered with a bipolar stimulating electrode (FHC) connected to a stimulation isolation unit (SIU91A, Cygnus Technology, Inc.). fEPSP recordings were obtained with a Multiclamp700A amplifier, digitized at 10 kHz with a Digidata 1440A, recorded with Clampex 10, and analyzed using Clampfit 10 software (Molecular Devices). Recordings were filtered online at 5 kHz with a Bessel low-pass filter.

I/O curves of fEPSPs were determined by gradually increasing the stimulus intensity every 15 s (10 to 130 μA in 10-μA steps). Paired-pulse ratio (PPR) was assessed by applying two pulses at various interstimulus intervals (ISIs: 10, 20, 30, 50, 100, and 200 ms). PPR was quantified as the ratio of the fEPSP slope of stimulus 2 to stimulus 1. Baseline responses were evoked every 30 s (0.033 Hz) using a stimulation intensity yielding 40 to 60% of the maximal response. The initial slope of the fEPSP (1-ms window) was used to assess changes in synaptic strength. Experiments in which there was a >5% drift in the response magnitude during the 20-min baseline period before LTP induction were excluded from further analysis. Small subthreshold long-term potentiation (subsaturating LTP) was induced with a "weak-TBS" consisting of three stimulus bursts (five pulses at 100 Hz/burst) separated by 200 ms. Data were normalized to the baseline response and LTP magnitude was quantified as % baseline response. LTP was measured by comparing the average response 50 to 60 min post-TBS to the average of the last 10 min of baseline. Statistical analyses were performed using each animal as an "n," with each animal represented by the mean of one to three slices.

Chemogenetic Inhibition. To induce DREADD-Gi expression in DH projections to the LS, we utilized an established chemogenetic approach (17, 69, 70). Briefly, rats received bilateral microinjections (1 μL/hemisphere) of AAVretro-pmSyn1-EBFP-Cre (Addgene; 51507) or AAV-Cre-GFP (UNC Vector Core) into the LS (5° angle: AP: −0.27 mm; ML: 1 mm; DV: −4.6 mm) and Cre-dependent DREADD (AAV2-hSyn-DIO-hM4D(Gi)-mCherry; Addgene; 44362) into the DH (10° angle: AP: −4.36 mm; ML: 3.4 mm; DV: −2.4 mm). All rats received a systemic injection of CNO (1 mg/kg, i.p.), to control for potential noninert aspects of CNO (71), 30 min prior to testing (72). Cre-mediated DREADD recombination was verified through immunofluorescence using primary antibodies anti-mCherry (1:250; Novus Biologicals; NBP2-25157) and anti-GFP (1:300; Abcam; ab13970).

Immunohistochemistry and Immunofluorescence. Two hours following testing, tissue was collected to quantify cFos expression (73) during maximal cFos expression following neuronal activity (74, 75). Rats were perfused through transcardial perfusion with PBS followed by 4% paraformaldehyde (PFA). Brains were immediately extracted and postfixed in 4% PFA for 2 h and then 30% sucrose in PBS for 48 h at 4 °C. Prior to sectioning, brains were frozen on dry ice. Coronal sections (20 μm) were cut on a cryostat (Leica), and every third section was collected. Fos immunostaining was performed as previously

published (76). Brain sections were blocked in 3% normal donkey serum with 0.3% Triton-X for 2 h after quenching with hydrogen peroxide. Sections were incubated overnight in a rabbit anti-Fos primary antibody (1:10 000; Millipore; PC38) followed by a 2-h incubation in a biotinylated donkey anti-rabbit secondary antibody (1:500; Jackson ImmunoResearch Laboratories; 711-065-152). Sections were then incubated for 2 h in an avidin–biotin complex solution (1:500, Vector Laboratories; PK-6101) before being reacted with 3,3′-diaminobenzidine (Sigma; D12384) in a Tris buffer, hydrogen peroxide, and nickel ammonium sulfate solution for cFos visual quantification. NeuN and IBA immunoreactivity in the DH was determined through immunofluorescence. Briefly, brain sections were blocked in 3% normal donkey serum with 0.3% Triton-X for 1 h at room temperature. Sections were then incubated at room temperature overnight in primary antibodies (anti-NeuN; 1:1,000; Millipore ; MAB377 or anti-IBA1; 1:500; Abcam; ab178846) diluted in PBS with 3% normal donkey serum and 0.3% Tween-20. Alexa Fluor 488- or 594-conjugated secondary antibodies were used at 1:500 (Jackson ImmunoResearch Laboratories, Inc.) and the numbers of NeuN and IBA1-immunoreactive cells were counted within the field of view at 10× magnification. cFos labeling was imaged and quantified by an individual blinded to treatment groups at 10× magnification using an Olympus IX51 research microscope with Micromanager software (version 1.4). Statistical analyses were performed using each animal as an "n," with each animal represented by the mean of two slices.

Statistical Analyses. Sample sizes were based on our previous publications (23–26). The standardized effect size was calculated using Cohen's d_s (77) in Excel 16.39 (Microsoft Corporation). Values >0.8 were interpreted as being of robust scale (*SI Appendix*, Table S2). All statistical analyses were performed using Prism 8 (GraphPad Software, Inc.). We used factorial analyses of variance (ANOVAs) or analyses of covariance (ANCOVA) where there were two variables. Significant main effects or interaction effects ($P < 0.05$) were followed with Fisher's predicted least-square difference (PLSD) post hoc comparisons. We only report significant effects that are important for data interpretation. Unpaired parametric t tests were used where there was one variable. Tests were two tailed except where directional hypotheses were deduced. We provide exact P values for those >0.0001. All data are presented as mean ± SEM.

Data Availability. All data needed to evaluate the conclusions in the paper are present in the paper and/or *SI Appendix*.

ACKNOWLEDGMENTS. This work was supported by the National Institute on Drug Abuse (NIDA; R01DA037257, S1-R01DA037257, and R21DA044486 to D.M.D., NIDA R21DA044486 to D.M.D.), National Institute of Neurological Disorders and Stroke (NINDS; F99NS108543 to J.A.M.), National Institute of General Medical Sciences (NIGMS; R25GM09545902 to The State University of New York at Buffalo) and Fundação de Amparo à Pesquisa do Estado de São Paulo (FAPESP; 2017/19284-0 to P.H.G.). The NIDA Drug Supply Program generously gifted the cocaine used in these studies.

1. A. J. Robison, E. J. Nestler, Transcriptional and epigenetic mechanisms of addiction. *Nat. Rev. Neurosci.* **12**, 623–637 (2011).
2. P. W. Kalivas, K. McFarland, Brain circuitry and the reinstatement of cocaine-seeking behavior. *Psychopharmacology (Berl.)* **168**, 44–56 (2003).
3. M. A. Parvaz, S. J. Moeller, R. Z. Goldstein, Incubation of cue-induced craving in adults addicted to cocaine measured by electroencephalography. *JAMA Psychiatry* **73**, 1127–1134 (2016).
4. X. Li, M. Venniro, Y. Shaham, Translational research on incubation of cocaine craving. *JAMA Psychiatry* **73**, 1115–1116 (2016).
5. L. Lu, J. W. Grimm, J. Dempsey, Y. Shaham, Cocaine seeking over extended withdrawal periods in rats: Different time courses of responding induced by cocaine cues versus cocaine priming over the first 6 months. *Psychopharmacology (Berl.)* **176**, 101–108 (2004).
6. J. W. Grimm, B. T. Hope, R. A. Wise, Y. Shaham, Neuroadaptation. Incubation of cocaine craving after withdrawal. *Nature* **412**, 141–142 (2001).
7. J. L. Neisewander *et al*., Fos protein expression and cocaine-seeking behavior in rats after exposure to a cocaine self-administration environment. *J. Neurosci.* **20**, 798–805 (2000).
8. M. E. Wolf, Synaptic mechanisms underlying persistent cocaine craving. *Nat. Rev. Neurosci.* **17**, 351–365 (2016).
9. M. A. Enoch *et al*., Expression of glutamatergic genes in healthy humans across 16 brain regions; altered expression in the hippocampus after chronic exposure to alcohol or cocaine. *Genes Brain Behav.* **13**, 758–768 (2014).
10. M. A. Enoch *et al*., GABAergic gene expression in postmortem hippocampus from alcoholics and cocaine addicts; corresponding findings in alcohol-naïve P and NP rats. *PLoS One* **7**, e29369 (2012).
11. D. C. Mash *et al*., Gene expression in human hippocampus from cocaine abusers identifies genes which regulate extracellular matrix remodeling. *PLoS One* **2**, e1187 (2007).
12. Z. Zhou, Q. Yuan, D. C. Mash, D. Goldman, Substance-specific and shared transcription and epigenetic changes in the human hippocampus chronically exposed to cocaine and alcohol. *Proc. Natl. Acad. Sci. U.S.A.* **108**, 6626–6631 (2011).
13. R. A. Fuchs *et al*., The role of the dorsomedial prefrontal cortex, basolateral amygdala, and dorsal hippocampus in contextual reinstatement of cocaine seeking in rats. *Neuropsychopharmacology* **30**, 296–309 (2005).
14. D. R. Ramirez *et al*., Dorsal hippocampal regulation of memory reconsolidation processes that facilitate drug context-induced cocaine-seeking behavior in rats. *Eur. J. Neurosci.* **30**, 901–912 (2009).
15. X. Xie, A. A. Arguello, A. M. Wells, A. M. Reittinger, R. A. Fuchs, Role of a hippocampal SRC-family kinase-mediated glutamatergic mechanism in drug context-induced cocaine seeking. *Neuropsychopharmacology* **38**, 2657–2665 (2013).
16. A. H. Luo, P. Tahsili-Fahadan, R. A. Wise, C. R. Lupica, G. Aston-Jones, Linking context with reward: A functional circuit from hippocampal CA3 to ventral tegmental area. *Science* **333**, 353–357 (2011).
17. E. M. McGlinchey, G. Aston-Jones, Dorsal Hippocampus drives context-induced cocaine seeking via inputs to lateral septum. *Neuropsychopharmacology* **43**, 987–1000 (2018).
18. A. M. Wells *et al*., Contribution of an SFK-mediated signaling pathway in the dorsal Hippocampus to cocaine-memory reconsolidation in rats. *Neuropsychopharmacology* **41**, 675–685 (2016).
19. R. A. Fuchs, J. L. Eaddy, Z. I. Su, G. H. Bell, Interactions of the basolateral amygdala with the dorsal hippocampus and dorsomedial prefrontal cortex regulate drug context-induced reinstatement of cocaine-seeking in rats. *Eur. J. Neurosci.* **26**, 487–498 (2007).
20. A. M. Wells *et al*., Interaction between the basolateral amygdala and dorsal hippocampus is critical for cocaine memory reconsolidation and subsequent drug context-induced cocaine-seeking behavior in rats. *Learn. Mem.* **18**, 693–702 (2011).
21. X. Xie, D. R. Ramirez, H. C. Lasseter, R. A. Fuchs, Effects of mGluR1 antagonism in the dorsal hippocampus on drug context-induced reinstatement of cocaine-seeking behavior in rats. *Psychopharmacology (Berl.)* **208**, 1–11 (2010).
22. X. Xie, A. M. Wells, R. A. Fuchs, Cocaine seeking and taking: Role of hippocampal dopamine D1-like receptors. *Int. J. Neuropsychopharmacol.* **17**, 1533–1538 (2014).
23. A. M. Gancarz *et al*., Activin receptor signaling regulates cocaine-primed behavioral and morphological plasticity. *Nat. Neurosci.* **18**, 959–961 (2015).
24. Z. J. Wang *et al*., BRG1 in the nucleus accumbens regulates cocaine-seeking behavior. *Biol. Psychiatry* **80**, 652–660 (2016).
25. C. T. Werner *et al*., E3 ubiquitin ligase Smurf1 in the nucleus accumbens mediates cocaine seeking. *Biol. Psychiatry* **84**, 881–892 (2018).
26. Z. J. Wang *et al*., Activin A is increased in the nucleus accumbens following a cocaine binge. *Sci. Rep.* **7**, 43658 (2017).
27. A. E. Kelley, Ventral striatal control of appetitive motivation: Role in ingestive behavior and reward-related learning. *Neurosci. Biobehav. Rev.* **27**, 765–776 (2004).
28. Y. Hasegawa *et al*., Acute modulation of synaptic plasticity of pyramidal neurons by activin in adult hippocampus. *Front. Neural Circuits* **8**, 56 (2014).
29. A. Kurisaki *et al*., Activin induces long-lasting N-methyl-D-aspartate receptor activation via scaffolding PDZ protein activin receptor interacting protein 1. *Neuroscience* **151**, 1225–1235 (2008).
30. C. T. Werner *et al*., Ubiquitin-proteasomal regulation of chromatin remodeler INO80 in the nucleus accumbens mediates persistent cocaine craving. *Sci. Adv.* **5**, eaay0351 (2019).
31. D. H. Epstein, K. L. Preston, The reinstatement model and relapse prevention: A clinical perspective. *Psychopharmacology (Berl.)* **168**, 31–41 (2003).
32. J. Jeong, M. Ahn, K. B. Sim, C. Moon, T. Shin, Immunohistochemical analysis of activin A expression in spinal cords of rats with clip compression injuries. *Acta Histochem.* **116**, 747–752 (2014).
33. H. Wilms *et al*., Regulation of activin A synthesis in microglial cells: Pathophysiological implications for bacterial meningitis. *J. Neurosci. Res.* **88**, 16–23 (2010).
34. T. Nakamura *et al*., Activin-binding protein from rat ovary is follistatin. *Science* **247**, 836–838 (1990).
35. R. L. Neve, K. A. Neve, E. J. Nestler, W. A. J. Carlezon Jr., Use of herpes virus amplicon vectors to study brain disorders. *Biotechniques* **39**, 381–391 (2005).
36. G. Krapivinsky *et al*., The NMDA receptor is coupled to the ERK pathway by a direct interaction between NR2B and RasGRF1. *Neuron* **40**, 775–784 (2003).
37. G. Fischer *et al*., Ro 25-6981, a highly potent and selective blocker of N-methyl-D-aspartate receptors containing the NR2B subunit. Characterization in vitro. *J. Pharmacol. Exp. Ther.* **283**, 1285–1292 (1997).
38. K. Deng *et al*., Whole-brain mapping of projection from mouse lateral septal nucleus. *Biol. Open* **8**, bio043554 (2019).
39. H. McLennan, J. J. Miller, The hippocampal control of neuronal discharges in the septum of the rat. *J. Physiol.* **237**, 607–624 (1974).
40. L. A. Cenquizca, L. W. Swanson, Analysis of direct hippocampal cortical field CA1 axonal projections to diencephalon in the rat. *J. Comp. Neurol.* **497**, 101–114 (2006).
41. L. Lu, J. W. Grimm, B. T. Hope, Y. Shaham, Incubation of cocaine craving after withdrawal: A review of preclinical data. *Neuropharmacology* **47**, 214–226 (2004).
42. A. Purgianto *et al*., Different adaptations in AMPA receptor transmission in the nucleus accumbens after short vs long access cocaine self-administration regimens. *Neuropsychopharmacology* **38**, 1789–1797 (2013).
43. M. E. Wolf, The Bermuda Triangle of cocaine-induced neuroadaptations. *Trends Neurosci.* **33**, 391–398 (2010).

44. D. W. Self, K. H. Choi, D. Simmons, J. R. Walker, C. S. Smagula, Extinction training regulates neuroadaptive responses to withdrawal from chronic cocaine self-administration. *Learn. Mem.* **11**, 648–657 (2004).
45. M. E. Wolf, C. R. Ferrario, AMPA receptor plasticity in the nucleus accumbens after repeated exposure to cocaine. *Neurosci. Biobehav. Rev.* **35**, 185–211 (2010).
46. H. C. Lasseter, X. Xie, D. R. Ramirez, R. A. Fuchs, Sub-region specific contribution of the ventral hippocampus to drug context-induced reinstatement of cocaine-seeking behavior in rats. *Neuroscience* **171**, 830–839 (2010).
47. C. T. Werner, M. T. Stefanik, M. Milovanovic, A. Caccamise, M. E. Wolf, Protein translation in the nucleus accumbens is dysregulated during cocaine withdrawal and required for expression of incubation of cocaine craving. *J. Neurosci.* **38**, 2683–2697 (2018).
48. M. T. Stefanik, M. Milovanovic, C. T. Werner, J. C. G. Spainhour, M. E. Wolf, Withdrawal from cocaine self-administration alters the regulation of protein translation in the nucleus accumbens. *Biol. Psychiatry* **84**, 223–232 (2018).
49. A. E. Lepack *et al*., Dopaminylation of histone H3 in ventral tegmental area regulates cocaine seeking. *Science* **368**, 197–201 (2020).
50. W. J. Wright *et al*., Silent synapses dictate cocaine memory destabilization and reconsolidation. *Nat. Neurosci.* **23**, 32–46 (2020).
51. C. L. Pickens *et al*., Neurobiology of the incubation of drug craving. *Trends Neurosci.* **34**, 411–420 (2011).
52. D. M. Walker *et al*., Cocaine self-administration alters transcriptome-wide responses in the brain's reward circuitry. *Biol. Psychiatry* **84**, 867–880 (2018).
53. E. S. Calipari *et al*., Synaptic microtubule-associated protein EB3 and SRC phosphorylation mediate structural and behavioral adaptations during withdrawal from cocaine self-administration. *J. Neurosci.* **39**, 5634–5646 (2019).
54. H. Ageta *et al*., Activin plays a key role in the maintenance of long-term memory and late-LTP. *Learn. Mem.* **17**, 176–185 (2010).
55. M. R. Müller, F. Zheng, S. Werner, C. Alzheimer, Transgenic mice expressing dominant-negative activin receptor IB in forebrain neurons reveal novel functions of activin at glutamatergic synapses. *J. Biol. Chem.* **281**, 29076–29084 (2006).
56. H. Y. Liu *et al*., Localisation and role of activin receptor-interacting protein 1 in mouse brain. *J. Neuroendocrinol.* **25**, 87–95 (2013).
57. A. M. Thompson, J. Swant, B. A. Gosnell, J. J. Wagner, Modulation of long-term potentiation in the rat hippocampus following cocaine self-administration. *Neuroscience* **127**, 177–185 (2004).
58. M. G. Kutlu, T. J. Gould, Effects of drugs of abuse on hippocampal plasticity and hippocampus-dependent learning and memory: Contributions to development and maintenance of addiction. *Learn. Mem.* **23**, 515–533 (2016).
59. Z. Dong *et al*., Hippocampal long-term depression mediates spatial reversal learning in the Morris water maze. *Neuropharmacology* **64**, 65–73 (2013).
60. A. M. Gancarz, M. A. Kausch, D. R. Lloyd, J. B. Richards, Between-session progressive ratio performance in rats responding for cocaine and water reinforcers. *Psychopharmacology (Berl.)* **222**, 215–223 (2012).
61. A. M. Gancarz-Kausch, D. N. Adank, D. M. Dietz, Prolonged withdrawal following cocaine self-administration increases resistance to punishment in a cocaine binge. *Sci. Rep.* **4**, 6876 (2014).
62. G. Paxinos, C. Watson, *The Rat Brain in Stereotaxic Coordinates*, (Elsevier, Burlington, MA, 2009).
63. A. Radiske *et al*., Requirement for BDNF in the reconsolidation of fear extinction. *J. Neurosci.* **35**, 6570–6574 (2015).
64. C. M. Johannessen *et al*., COT drives resistance to RAF inhibition through MAP kinase pathway reactivation. *Nature* **468**, 968–972 (2010).
65. H. Ageta *et al*., Activin in the brain modulates anxiety-related behavior and adult neurogenesis. *PLoS One* **3**, e1869 (2008).
66. H. B. Yang *et al*., cAMP-dependent protein kinase activated Fyn in spinal dorsal horn to regulate NMDA receptor function during inflammatory pain. *J. Neurochem.* **116**, 93–104 (2011).
67. A. Rodenas-Ruano, A. E. Chávez, M. J. Cossio, P. E. Castillo, R. S. Zukin, REST-dependent epigenetic remodeling promotes the developmental switch in synaptic NMDA receptors. *Nat. Neurosci.* **15**, 1382–1390 (2012).
68. C. R. Ferrario *et al*., Alterations in AMPA receptor subunits and TARPs in the rat nucleus accumbens related to the formation of Ca^{2+}-permeable AMPA receptors during the incubation of cocaine craving. *Neuropharmacology* **61**, 1141–1151 (2011).
69. I. F. Augur, A. R. Wyckoff, G. Aston-Jones, P. W. Kalivas, J. Peters, Chemogenetic activation of an extinction neural circuit reduces cue-induced reinstatement of cocaine seeking. *J. Neurosci.* **36**, 10174–10180 (2016).
70. R. C. Twining, J. E. Vantrease, S. Love, M. Padival, J. A. Rosenkranz, An intra-amygdala circuit specifically regulates social fear learning. *Nat. Neurosci.* **20**, 459–469 (2017).
71. D. A. MacLaren *et al*., Clozapine N-oxide administration produces behavioral effects in long-evans rats: Implications for designing DREADD experiments. *eNeuro* **3**, ENEURO.0219-16.2016 (2016).
72. A. H. Runegaard *et al*., Locomotor- and reward-enhancing effects of cocaine are differentially regulated by chemogenetic stimulation of Gi-signaling in dopaminergic neurons. *eNeuro* **5**, ENEURO.0345-17.2018 (2018).
73. X. Li *et al*., Role of anterior intralaminar nuclei of thalamus projections to dorsomedial striatum in incubation of methamphetamine craving. *J. Neurosci.* **38**, 2270–2282 (2018).
74. R. Müller, R. Bravo, J. Burckhardt, T. Curran, Induction of c-fos gene and protein by growth factors precedes activation of c-myc. *Nature* **312**, 716–720 (1984).
75. S. T. Young, L. J. Porrino, M. J. Iadarola, Cocaine induces striatal c-fos-immunoreactive proteins via dopaminergic D1 receptors. *Proc. Natl. Acad. Sci. U.S.A.* **88**, 1291–1295 (1991).
76. E. M. McGlinchey, M. H. James, S. V. Mahler, C. Pantazis, G. Aston-Jones, Prelimbic to accumbens core pathway is recruited in a dopamine-dependent manner to drive cued reinstatement of cocaine seeking. *J. Neurosci.* **36**, 8700–8711 (2016).
77. J. Cohen, *Statistical Power Analysis for the Behavioral Sciences*, (Lawrence Earlbaum, Hillsdale, New Jersey, 1988).